Modeling Conventional Swing of a Cricket Ball Using COMSOL Multiphysics ®

Richie Latchman Akash Pooransingh
Department of Electrical and Computer Engineering
The University of the West Indies, St. Augustine Campus
Email: richielatchman@hotmail.com, akash.pooransingh@sta.uwi.edu

Abstract: The commercialization of cricket has increased the stakes for all involved. Conventional swing is one phenomenon which a bowler uses to gain an advantage over the batsman. This study involved simulating conventional swing in the CFD module of COMSOL Multiphysics® and comparing the simulated results with experimental results of previous researchers. The variation in the side and drag forces on the ball were investigated by varying the velocity, seam angle and backspin of the ball. The fluid flow profile in the simulated results were as expected, however, there was no transition region for higher ball velocities where it was expected the side force coefficient would fall to a lower constant value. The results and further investigation seem to suggest that the k-ε turbulence model may not suitable for simulating the flow around a cricket ball accurately or that the turbulence model parameters need to be redefined for this application.

Keywords: CFD, k-ε turbulence model.

1. Introduction

There are numerous studies in which the aerodynamics of a cricket ball and the respective forces and coefficients were determined experimentally. Alam et al. (2007) utilized a wind tunnel and a six component sensor to measure the aerodynamic forces on the cricket ball. The aerodynamic forces and moments were measured for a range of velocities and seam orientation. By using video and still images the airflow around the cricket ball was visualized and documented. Barton (1982) conducted experiments in which old and new balls were mounted on a pendulum. He also performed experiments in which the cricket ball was rolled down a ramp (to create spin) and then into a wind tunnel flow. The side force on the ball was indirectly calculated from trajectory measurements of the ball.

Computational fluid dynamics (CFD) is an integration of mathematics, fluid dynamics and computer science. CFD can be used as a research tool to perform numerical investigations that are analogous to wind-tunnel experiments. With the increased performance power of computer hardware and the development of scientifically validated computational fluid dynamics (CFD) modelling tools, analyzing a complex flow problem such as that over the cricket ball may be possible with great accuracy. (Bandara and Rathnayanka 2012) There are numerous advantages in using a CFD approach. By using CFD, there is a considerable reduction in the lead times and costs when compared to an experimental-based approach. CFD provides the capability to solve a range of complex flow problems in which the analytical approach may be deficient. CFD also provides comprehensive and visual information that may not be possible with experimental and analytical fluid dynamics (Jiyuan, Yeoh and Liu 2008,4 -5).

Bandara and Rathnayanka (2012) adopted a CFD approach to investigate the aerodynamic forces on a cricket ball during conventional swing. Their study is, however, confined to the analysis of a non-spinning cricket ball. This study will adopt a CFD approach using COMSOL Multiphysics® to analyze the flow around a cricket ball during conventional swing for the cases of a non-spinning and spinning ball.

2. Theory

Conventional Swing

Fast bowlers carefully use the primary seam to make the cricket ball swing. They release the ball with the seam at an angle to the initial line of flight. Once the Reynolds number (Re) is within a specific range, the boundary layer is “tripped” into turbulence by the seam on one side of the ball while the boundary layer on the non-seam side remains laminar.

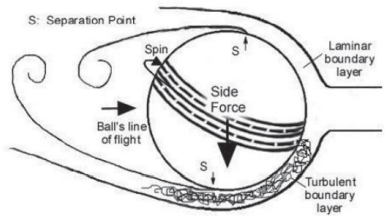

Figure 1 Schematic of flow over a cricket ball for conventional swing (Mehta 2008)

The turbulent boundary layer separates later than the laminar boundary layer. This creates a pressure differential which produces a side force on the ball.

To investigate conventional swing, Mehta (2008) conducted experiments to verify that an asymmetric boundary layer separation on a cricket ball leads to a pressure differential across it. Figure 2 shows the measured pressures on a ball mounted in a wind tunnel with the seam angled at 20° to the oncoming flow.

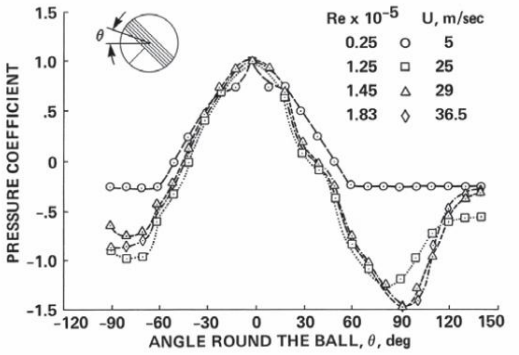

Figure 2 Pressure distributions on a cricket ball held at a seam angle of 20 degrees (Mehta 2008)

3. Method and Use of COMSOL Multiphysics

3.1 Pre-process of the CFD Analysis

3.1.1 Creation of the computational model of a cricket ball and the computational domain.

A computational model of a cricket ball and the computational domain were built using the geometry node of the model builder in the CFD module.

The geometry of the computational model of the cricket ball was simplified for better meshing and to reduce the computational demands of the simulations. Using law number 5 of International Cricket Council regulations and the British Standard BS5993, the cricket ball was modelled as a sphere of diameter 72 mm with the primary seam incorporated as a 20 mm wide concentric rim projecting 1 mm from the ball surface. The mass of the ball was taken as 0.160 kg.

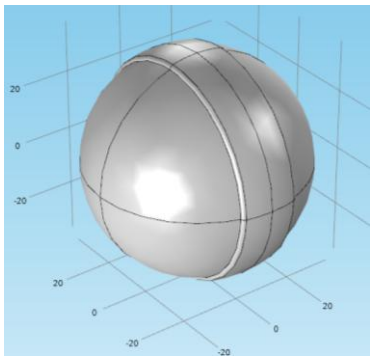

Figure 3 Computational model of the cricket ball built in COMSOL Multiphysics

The cricket ball was modelled as a homogeneous single material since the composite nature of the actual cricket ball has no effect on the development of the fluid flow profile around the ball. The defining criterion for fluid flow profile is the geometrical shape of the ball.

An important aspect of CFD analysis is the definition and creation of the geometry for the flow region (i.e. the computational domain). In the creation of the computational domain for CFD calculations, it must allow the flow dynamics to be sufficiently developed across its length. For the cricket ball flow analysis, it is required to capture the occurrence of complex wake-making development that persists behind the ball as the flow passes over the ball. The top and bottom boundary effects may influence the flow passing over the ball. The height of the domain needs to be prescribed at a distance to sufficiently remove any of these boundary effects on the fluid flow surrounding the ball, but still manageable for CFD calculations (Jiyuan, Yeoh and Liu 2008, 35). According to Bandara and Rathnayanka (2012), the computational domain should be represented by a rectangular parallelepiped having dimensions of 400 mm x

600 mm x 400 mm in the x, y and z directions respectively. The computational model of the ball is to be placed at a distance of 150 mm from the inlet boundary to capture the downstream effects effectively.

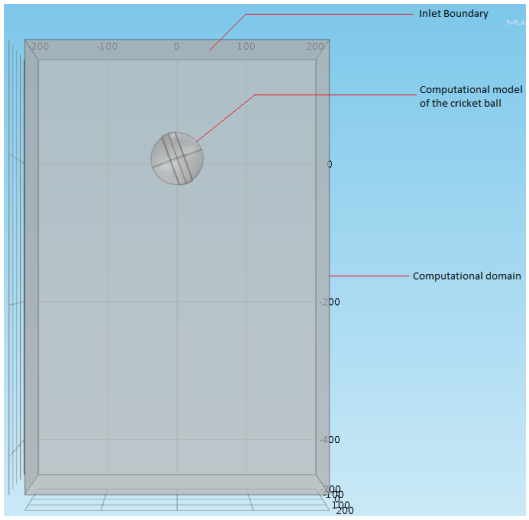

Figure 4 Computational model of the cricket ball positioned at 150 mm from the inlet boundary of the computational domain

3.1.2 Mesh Generation

For 2-D and 3-D simulations triangular cells and tetrahedral cells were used respectively for mesh generation. For the simulations performed, very coarse meshes for the computational model and computational domain were used as the starting point. The mesh for the computational model and computational domain were refined to obtain the most accurate solution within limitations of the computational demand and calculation turnover time requirements. The elements in the mesh of the computational domain were calibrated for fluid dynamics while the elements in the mesh of the computational model of the cricket ball were calibrated for general physics.

3.1.3 Selection of Fluid Properties and Physics

The fluid through which the cricket ball travels is air, which is regarded as a Newtonian fluid. The Mach number of air is less than 0.3. (COMSOL 2013, 84)

The driving force of conventional swing is based on the principle that as the ball travels through air there is turbulent flow on one side of the ball while there is laminar flow on the other side (Figure 2). A turbulent flow interface was therefore used to model the flow around the cricket ball. The Turbulent Flow, k-ε interface was used to simulate the flow for a non-rotating ball while the Rotating Machinery, Turbulent Flow, k-ε user interface was used for simulating flows in which backspin of the ball was considered. The *k*-ε model is one of the most widely used and valid turbulence models with its performance assessed against a number of practical flows. Bandara and Rathnayanka (2012) also used this model in their study of modelling conventional swing with CFD.

3.1.4 Specification of Boundary Conditions

In modelling the fluid flow around the computational model of the cricket ball, the principle used in wind tunnel testing was simulated. That is, the fluid flow profile developed around a moving object at a specified velocity in still air is the same as that of moving air of the same velocity over a stationary object. (NASA 2014)

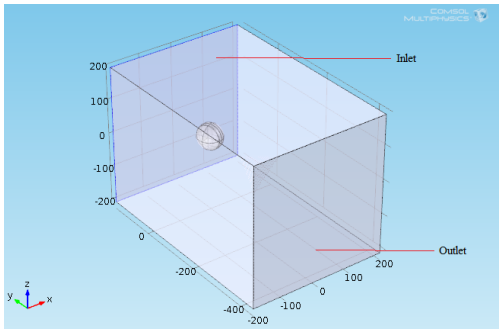

Figure 5 Inlet and outlet boundaries for the computational domain

Figure 5 shows the inlet and outlet boundaries for the computational domain. The remaining four surfaces of the computational domain are open boundaries.

Based on the model proposed by Marino Miccio Chemical Engineer (2014) in modelling the flow around a sphere, the following boundary conditions were specified for modelling the flow around the cricket ball.

- The inlet condition was specified by a normal inflow velocity. This velocity was the initial velocity at which the ball is bowled.
- The outlet condition was specified by a pressure on the outlet. The pressure at the outlet was 0 Pa.
- A symmetry boundary condition was specified for the open boundaries.

3.2 Modeling Strategy

The fluid flow simulation over a cricket ball is computationally demanding, therefore a multi-stage modelling strategy was implemented. Complexities were introduced gradually so that the influence of each alteration of the model was analyzed before introducing new complexities. Complexities in the modelling process were introduced step by step in order to achieve the best accuracy possible within limitations. The complexities included changes to the geometry, the physical properties, and in the description of the governing equations. A 2D representation of a cross-section of the cricket ball geometry was used to give initial estimates of the flow field that was used when setting up the full 3D model. A simplified model of the cricket ball being a uniform sphere was the starting point of the 3D modelling process. The work of previous researchers suggest that resultant side force on a cricket ball is dependent of three parameters, the velocity of the ball, the angle of the seam and the backspin of the ball.

The variation in side force for a still ball (no backspin) was investigated for varying seam angles and velocity. The seam angle will be altered from 0° to 30° at increments of 10°. For each seam angle simulations will be run for velocities from 50mph to 100 mph at increments of 5 mph. The velocity of 67 mph will be included since this according to Mehta is the velocity for maximum swing at an angle of 20°

3.3 Post process of the CFD Analysis

The CFD module of COMSOL Multiphysics generates three types of plots for the results of a simulation.

1. Velocity magnitude – illustrates the flow velocity around the ball.
2. Surface contour of pressure – illustrates the pressure distribution.
3. Wall resolution – the wall lift-off plot can be used to check the accuracy of the solution.

3.3.1 Determination of the drag force and side force

The drag and side forces on the ball were determined by finding the surface integral of the pressure distribution on the respective surfaces of the ball. This was done by using the derived values function in the CFD module.

4. Governing Equations

The Navier Stokes equations in their most general form are given by:

The continuity equation that represents the conservation of mass :

$$\frac{\partial \rho}{\partial t} + \nabla \cdot (\rho \boldsymbol{u}) = 0$$

Vector equation that represents the conservation of momentum:

$$\rho \frac{\partial \boldsymbol{u}}{\partial t} + \rho(\boldsymbol{u} \cdot \nabla)\boldsymbol{u} = \nabla \cdot [-p\boldsymbol{I} + \tau] + \boldsymbol{F}$$

The Reynolds-Averaged Navier-Stokes (RANS) Equations for an incompressible and Newtonian fluid are given by

$$\rho \frac{\partial \boldsymbol{u}}{\partial t} + \rho(\boldsymbol{u} \cdot \nabla)\boldsymbol{u} = \nabla \cdot [-p\boldsymbol{I} + \mu(\nabla \boldsymbol{u} + (\nabla \boldsymbol{u})^T)] + \boldsymbol{F}$$

$$\rho \nabla \cdot \boldsymbol{u} = 0$$

The *k*-ε model introduces two additional transport equations and two dependent variables: the turbulent kinetic energy, k, and the dissipation rate of turbulence energy, ε. The turbulent viscosity is modeled by

$$\mu_T = \rho C_\mu \frac{k^2}{\varepsilon}$$

Where C_μ is a model constant.

The transport equation for k is:

$$\rho \frac{\partial k}{\partial t} + \rho \boldsymbol{u} \cdot \nabla k = \nabla \left(\left(\mu + \frac{\mu_T}{\sigma_k} \right) \nabla k \right) + P_k - \rho \varepsilon$$

Where the production term is

$$P_k = \mu_T \left(\nabla \boldsymbol{u} : (\nabla \boldsymbol{u} + (\nabla \boldsymbol{u})^T) - \frac{2}{3}(\nabla \cdot \boldsymbol{u}^2) \right) - \frac{2}{3} \rho k \nabla \cdot \boldsymbol{u}$$

The transport equation for ε reads:

$$\rho\frac{\partial\varepsilon}{\partial t}+\rho\boldsymbol{u}\cdot\nabla\varepsilon=\nabla\cdot\left(\left(\mu+\frac{\mu_T}{\sigma_\varepsilon}\right)\nabla\varepsilon\right)+C_{\varepsilon1}\frac{\varepsilon}{k}P_k-C_{\varepsilon2}\rho\frac{\varepsilon^2}{k}$$

The model constants in the above equations are determined from experimental data

Table 1: Model constants for Turbulent Flow, *k*-ε interface

Constant	Value
C_μ	0.09
$C_{\varepsilon1}$	1.44
$C_{\varepsilon2}$	1.92
σ_k	1.0
σ_ε	1.3

$$d\boldsymbol{x}=d\boldsymbol{x}(r_{bp},\omega,t^*)$$

$\omega=2\pi\omega t^*$, t^* = Frozen time

5. Results

5.1 Still Ball Flow Profile Analysis

5.1.1 2 D Models

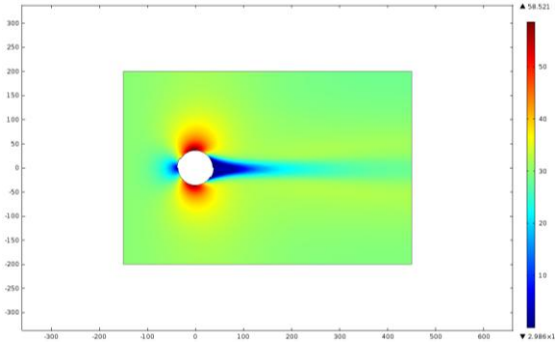

Figure 6. Velocity magnitude plot for a 2D simulation model of the cricket ball and computational domain using extremely fine and finer predefined elements respectively

The velocity magnitude plot in Figure 6 displays a profile that was expected. There exists a stagnation point at the front of the ball. In this region the velocity of the air is approximately zero. As the air flows around the surface of the ball, the velocity of the fluid increases due to compression. It can be seen that there is a larger region of high velocity on the seam side of the ball. This can be attributed to the seam "tripping" the fluid into turbulence. The region of fluid immediately behind the ball is at approximately zero velocity due to boundary layer separation on either side of the ball. The difference in the velocity profile on either side of the ball will correspond to a difference in pressure, as illustrated in Figure 7. It can be seen that the pressure of the fluid on the seam side is greater than on the non-seam side. This proves that the resultant side force on the ball is toward the seam side and therefore the ball will swing towards the seam side as expected.

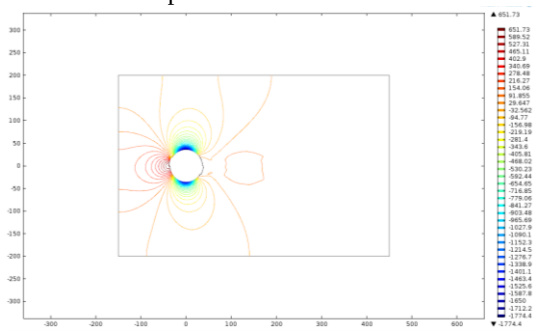

Figure 7. Pressure contour plot for a 2D simulation model of the cricket ball and computational domain using extremely fine and finer predefined elements respectively

5.1.2 3D Models

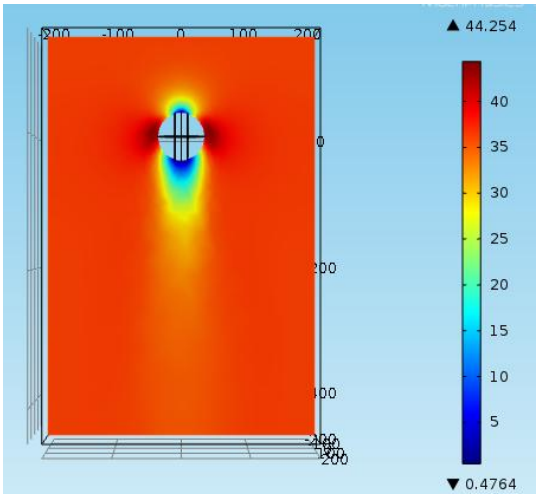

Figure 8. Velocity magnitude plot for a 3D simulation of a still ball at a seam angle of 0°

The flow profile of the 3D computational model illustrated in Figure 9 exhibits similar characteristics to that of the 2D model in Figure 6. The significant difference is the wake in the 3D model is deflected toward the non seam side. The deflection is owed to the fact that the flow

on the seam side is tripped into turbulence while the non-seam side remains laminar for the velocity of the air at which the simulation was conducted. The turbulent boundary layer separates at a point further behind the ball than the laminar layer, hence the deflection.

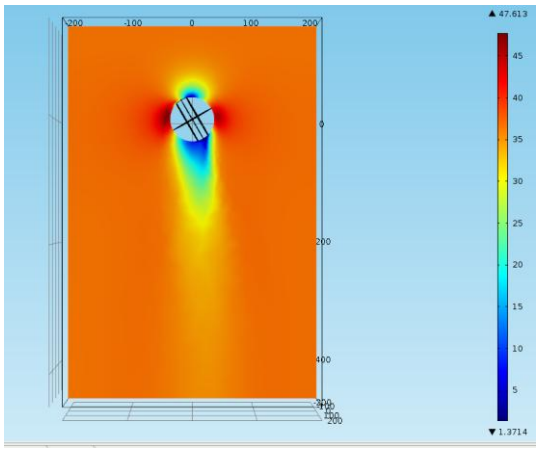

Figure 9. Velocity magnitude plot for a 3D simulation of a still ball at a seam angle of 20°

5.2 Still Ball Force Analysis

5.2.1 Variation in side force coefficient for varying seam angle and ball velocity

Table 2. Side force and side force coefficients for varying seam angles and ball velocity modeled in the k-epsilon turbulence interface**.**

	Side Force / N			Side Force Coefficient, C_S		
Seam Angle	**10°**	**20°**	**30°**	**10°**	**20°**	**30°**
Vel. / mph						
50	0.131	0.255	0.467	0.109	0.213	0.390
55	0.159	0.308	0.565	0.110	0.213	0.390
60	0.189	0.365	0.672	0.110	0.212	0.390
65	0.222	0.429	0.789	0.110	0.212	0.390
67	0.236	0.455	0.838	0.110	0.212	0.390
70	0.257	0.497	0.915	0.110	0.212	0.390
75	0.314	0.570	1.050	0.117	0.212	0.390
80	0.336	0.649	1.194	0.110	0.212	0.390
85	0.379	0.733	1.349	0.110	0.212	0.390
90	0.425	0.820	1.513	0.110	0.212	0.390
95	0.473	0.915	1.685	0.109	0.212	0.390
100	0.524	1.012	1.868	0.109	0.211	0.390

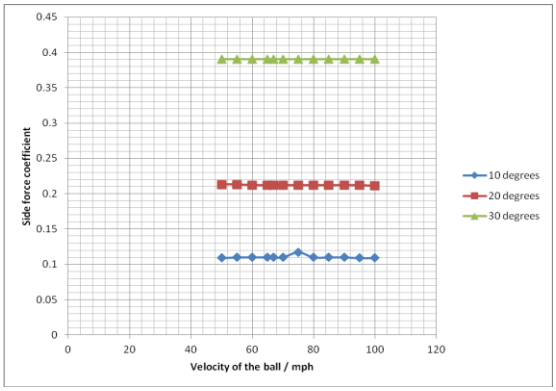

Figure 10. Graph showing the variation of the side force coefficient for differing velocities and seam angles

Analysis of the data in Table 2 and Figure 10 illustrates the following.

1. The side force on the ball increases as the velocity of the ball increases.
2. For the same velocity, the side force increases with increasing seam angle.
3. The side force coefficient remains approximately constant for increasing velocity for a particular seam angle.
4. The side force coefficient increases as the seam angle is increased.

5.3 Rotating Ball Flow Profile Analysis

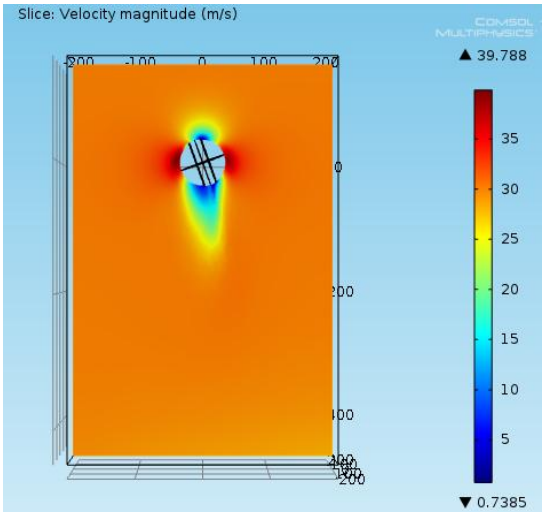

Figure 11. Velocity magnitude plot showing the flow profile for rotating ball at a velocity of 67 mph, seam angle of 20° and backspin rate of 11.4

The flow profile illustrated in Figure 11 exhibits similar characteristics to that Figure 9. The significant difference is in the wake, this can be attributed to the rotation of the ball.

5.4 Rotating Ball Force Analysis

5.4.1 Variation in side force coefficient for varying ball velocity and back spin rates

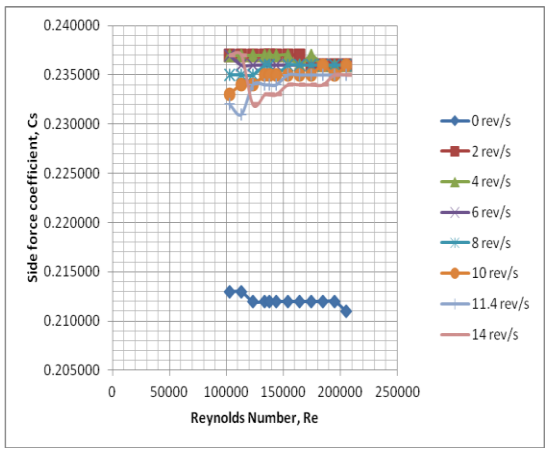

Figure 12. Graph showing the variation of the side force coefficient at varying backspin rates for a seam angle of 20°

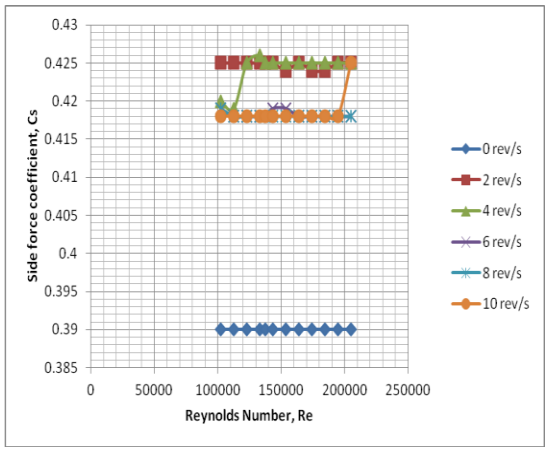

Figure 13. Graph showing the variation of the side force coefficient at varying backspin rates for a seam angle of 30°

Figures 12 and 13 show that the side force coefficient increases when there is back spin on the ball. The results indicate that the value of side coefficient is approximately similar for the different rates of backspin. It can be seen that the side force coefficient for all cases increases when the seam angle is increased from 20° to 30°.

6. Conclusions

Experimental data of previous research suggests that the side force and hence the amount of swing or lateral displacement is dependent on three key parameters, ball velocity, seam angle and back spin rate. In this study the side force experienced by a cricket ball model was investigated by varying the three key parameters in simulations done in the CFD module of COMSOL Multiphysics. The results showed moderate agreement with the principles suggested by previous researchers, namely the flow velocity profile and increase in side force coefficient with backspin. There could be no clear indication of the variation in side force for varying seam angles. In the simulations conducted, no case showed the expected transition region in which the side force coefficient reduced for higher ball velocity to a constant lower value. The results and further investigations seem to suggest that the k-ε turbulence model may not be suitable for simulating the fluid flow around a cricket ball or that the model constants need to be redefined for this application. It must be noted that due to limitations of computational performance requirements and simulation time that there were inaccuracies due to the fact the finest possible mesh element was not utilized for performing the simulations. .

7. References

1. Alam, F., R. La Brooy, S. Watkins and A. Subic, An experimental study of cricket ball aerodynamics, *In Proceedings of the International Conference on Mechanical Engineering*, (ICME2007)

2. Barton, N. G, On the swing of a cricket ball in flight. *Proc. R. Soc. Lond. A*, 109–131 (1982)

3. Bandara, R. M. P. S., and N. S. Rathnayaka, Modelling of Conventional Swing of the Cricket Ball using Computational Fluid Dynamics, *KDU International Symposium 2012*, 447- 457 (2012)

4. COMSOL, CFD Module User's Guide Version 4.3b (2013)

5. Marino Miccio Chemical Engineer, COMSOL: Flow Around A Sphere, (2014) Accessed March 20, 2015. http://marinomiccio.wix.com/home

6. Mehta, Rabindra, *Sports ball aerodynamics*, Springer Vienna, USA (2008)

7. Tu, Jiyuan, Guan Heng Yeoh and Chaoqun Liu, *Computational Fluid Dynamics: A Practical Approach*, 4 – 35, Elsevier, Oxford (2008)